



# The Electron Neutrino Mass Measurement by the HOLMES experiment

A Status Report

Andrea Giachero

*on behalf of HOLMES collaboration*

*University and INFN of Milano Bicocca*

June 6, 2014





## Known facts

- Neutrino are fermions;
- There are 3 active neutrino flavors ( $\nu_e, \nu_\mu, \nu_\tau$ );
- Neutrino flavor states are mixture of mass states ( $\nu_1, \nu_2, \nu_3$ );

⇒ neutrino oscillation

⇓

$$\delta m_{ij}^2 = |m_i^2 - m_j^2|$$

$$\sin^2 \theta_{ij} = f(|U_{ij}|^2)$$

$$|\nu_\alpha\rangle = \sum_j U_{\alpha j} |\nu_j\rangle$$

$$\left\{ \begin{array}{l} |\nu_\alpha\rangle : \text{Flavor weak eigenstate;} \\ U_{\alpha j} : \text{Neutrino mixing matrix;} \\ |\nu_j\rangle : \text{Mass eigenstate.} \end{array} \right.$$

Parameter	Best fit	$1\sigma$ range	$\sigma_{\text{symmetric}}$
$\mathcal{NH}$			
$\sin^2(\theta_{12})$	$3.08 \cdot 10^{-1}$	$(2.91 - 3.25) \cdot 10^{-1}$	$0.17 \cdot 10^{-1}$
$\sin^2(\theta_{13})$	$2.34 \cdot 10^{-2}$	$(2.16 - 2.56) \cdot 10^{-2}$	$0.22 \cdot 10^{-2}$
$\delta m^2$ [eV <sup>2</sup> ]	$7.54 \cdot 10^{-5}$	$(7.32 - 7.80) \cdot 10^{-5}$	$0.26 \cdot 10^{-5}$
$\Delta m^2$ [eV <sup>2</sup> ]	$2.44 \cdot 10^{-3}$	$(2.38 - 2.52) \cdot 10^{-3}$	$0.08 \cdot 10^{-3}$
$\mathcal{IH}$			
$\sin^2(\theta_{12})$	$3.08 \cdot 10^{-1}$	$(2.91 - 3.25) \cdot 10^{-1}$	$0.17 \cdot 10^{-1}$
$\sin^2(\theta_{13})$	$2.39 \cdot 10^{-2}$	$(2.18 - 2.60) \cdot 10^{-2}$	$0.21 \cdot 10^{-2}$
$\delta m^2$ [eV <sup>2</sup> ]	$7.54 \cdot 10^{-5}$	$(7.32 - 7.80) \cdot 10^{-5}$	$0.26 \cdot 10^{-5}$
$\Delta m^2$ [eV <sup>2</sup> ]	$2.40 \cdot 10^{-3}$	$(2.33 - 2.47) \cdot 10^{-3}$	$0.07 \cdot 10^{-3}$

Results of the global 3ν oscillation analysis [1, 2]

$$\left\{ \begin{array}{l} \delta m^2 = m_2^2 - m_1^2 \\ \Delta m^2 = m_3^2 - \frac{m_1^2 + m_2^2}{2} \end{array} \right.$$

Parameter	Dominated by [1]
$\theta_{12}$	Solar data
$\theta_{13}$	Short-baseline (SBL) reactor data Daya Bay, RENO
$\theta_{23}$	Atmospheric data Super-Kamiokande
$\delta m^2$	Long-baseline (LBL) accelerator data KamLAND
$\Delta m^2$	Long-baseline (LBL) accelerator data MINOS, T2K

# Neutrino mass hierarchy

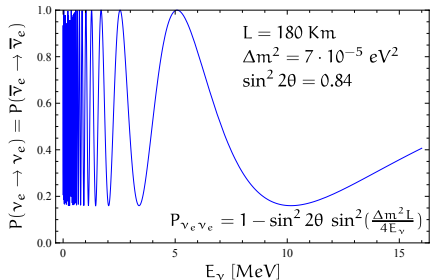
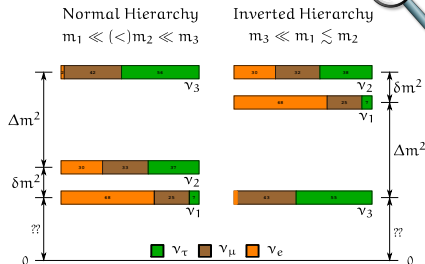


## Unknown facts

- Mass scale:
  - Mass of the lightest neutrino
- Mass ordering (hierarchy):
  - degenerate ( $\mathcal{QD}$ ):  $m_1 \simeq m_2 \simeq m_3$
  - normal ( $\mathcal{NH}$ ):  $m_1 \ll (<) m_2 \ll m_3$
  - inverted ( $\mathcal{IH}$ ):  $m_3 \ll m_1 \lesssim m_2$
- Mass Nature:
  - Dirac particle:  $\nu \neq \bar{\nu}$
  - Majorana particle:  $\nu = \bar{\nu}$
- Others?

## Oscillations experiments:

- Sensitive **ONLY** to the squared mass differences:  $\delta m_{ij}^2$ ;
- **NO** information about absolute mass scale and nature.



S. Goswami *et al.* [3]



## Constraint from cosmology:

- Cosmic microwave background (CMB);
- Galaxy clustering;
- Lyman-alpha forest;
- Weak lensing.

Observable	$m_{\Sigma} = \sum_k m_{\nu_k}$
Best limit	$m_{\Sigma} \leq 0.23 \text{ eV @ 95\% [4]}$

## Constraint from the Neutrinoless Double Beta-Decay ( $0\nu\beta\beta$ ):

- Forbidden by Standard Model ( $\Delta L = 2$ );
- Allowed only for Majorana neutrino;
- Never observed.
- $[\tau_{1/2}^{0\nu}]^{-1} = G^{0\nu} |M^{0\nu}|^2 |\langle m_{\beta\beta} \rangle|^2$

Decay	$(A, Z) \rightarrow (A, Z + 2) + 2e^{-}$
Observable	$m_{\beta\beta} =  \sum_k m_{\nu_k} U_{ek}^2 $
Best limit	$m_{\beta\beta} (^{76}\text{Ge}) \leq (200 \div 400) \text{ meV [5]}$ $m_{\beta\beta} (^{136}\text{Xe}) \leq (190 \div 450) \text{ meV [6]}$

$m_{\beta\beta}$ : Effective Majorana Mass

## Constraint from the Direct Neutrino Mass Determination:

- Kinematical analysis of the end point region of the  $\beta$  decay spectra;
- The neutrino is not directly observed but the energy of the decay products is precisely measured;

Decay	$(A, Z) \rightarrow (A, Z + 1) + e^{-} + \bar{\nu}_e$ ( $\beta D$ ) $(A, Z) + e^{-} \rightarrow (A, Z - 1) + \nu_e$ ( $EC$ )
Observable	$m_{\beta} = \sqrt{\sum_k m_{\nu_k}^2  U_{ek} ^2}$
Best limit	$m_{\beta} \leq 2.2 \text{ eV [7, 8]}$





Tool	Cosmology	Double Beta Decay	Beta Decay End Point
Observable	$m_{\Sigma} = \sum_k m_{\nu_k}$	$m_{\beta\beta} =  \sum_k m_{\nu_k} U_{ek}^2 $	$m_{\beta} = \sqrt{\sum_k m_{\nu_k}^2  U_{ek} ^2}$
Present Sensitivity	$\simeq 0.1$ eV	$\simeq 0.1$ eV	2 eV
Future Sensitivity	0.01 eV	0.01 eV	0.2 eV
Model Dependency	yes ☹️	yes ☹️	no ☺️
Systematics	large ☹️	small ☺️	large ☹️

## Cosmology

- The parameter  $m_{\Sigma}$  suffers of cosmological model dependency;

## Neutrinoless Double Beta

- The calculations of nuclear matrix elements of  $0\nu\beta\beta$ -decay is a challenge for nuclear physics (several different approach, model dependency).

## Beta Decay end-point measurement

- The measurement of the end point of nuclear beta or electron capture (EC) decays spectra is the only model-independent.

# Direct neutrino mass measurements

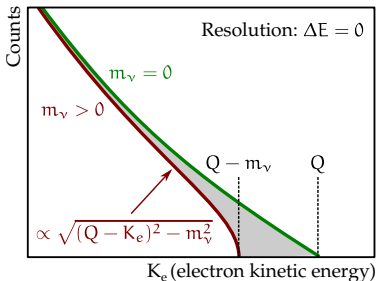


## Kinematics of weak decays with $\nu$ emission:

- only energy and momentum conservation;
- no further assumptions;
- low Q nuclear beta decays ( ${}^3\text{H}$ ,  ${}^{187}\text{Re}$ );

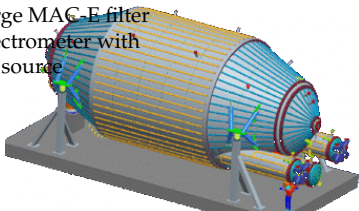
## Two approaches with different:

- **Spectrometry**: the  $\beta$  source is outside the spectrometry detector;
- **Calorimetry**: the  $\beta$  source is contained in the calorimetry detector which measures all the energy released except the  $\nu$  energy.

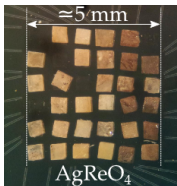


## Spectrometry: KATRIN

Large MAC-E filter spectrometer with  ${}^3\text{H}$  source



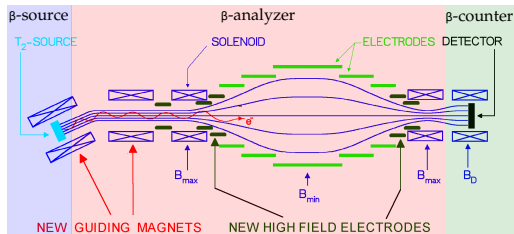
## Calorimetry: Mare, ECHO, Holmes



Array of low temperature microcalorimeters with  ${}^{187}\text{Re}$  or  ${}^{163}\text{Ho}$



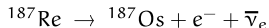
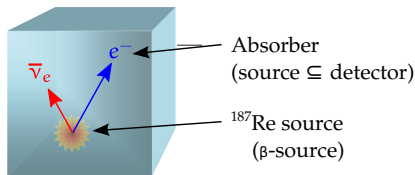
## Spectrometers: source $\neq$ detector



(Mainz spectrometer sketch-up from C. Kraus *et al.* [9])

- Tritium  $\beta$  decay:  
 ${}^3\text{H} \rightarrow {}^3\text{He}^+ + e^- + \bar{\nu}_e$
- Magnetic spectrometers and MAC-E filter [10];
- The  $\beta$ -electrons with enough energy to pass the MAC-E filter are detected;

## Calorimeters: source $\subseteq$ detector



- The  $\beta$  source is embedded in the detector (absorber);
- Ideally measurement of all the energy  $E$  released in the decay except for the  $\nu_e$  energy;



# Calorimeters vs Spectrometers

## General experimental requirements:

- High statistics at the beta spectrum end-point:
  - Low end-point energy  $Q$ :  $F(\delta E) \propto (\delta E/Q)^3$   
 $\Rightarrow$  where  $\delta E$  is the energy range considered near the end point;
  - High source activity and high efficiency;
- High energy resolution  $\Delta E$  (same order of magnitude of  $m_\nu$  sensitivity);
- High signal-to-noise ratio (SNR);
- Small systematic effects.

## Spectrometers: source $\neq$ detector:

- ☺ high statistics:  $\tau_{1/2}({}^3\text{H}) = 12.3 \text{ y}$ ;
- ☺ high energy resolution:  $\delta E \simeq 1 \text{ eV}$ ;
- ☹ systematics due to source effect;
- ☹ systematics due to decay to excited states;
- ☹ background.

## Calorimeters: source $\subseteq$ detector:

- ☺ no backscattering;
- ☺ no energy losses in the source;
- ☺ no solid state excitation;
- ☺ no atomic/molecular final state effect;
- ☹ limited statistics:  $\tau_{1/2}({}^{187}\text{Re}) \simeq 4 \cdot 10^{10} \text{ y}$ ;
- ☹ systematics due to pile-up;
- ☹ background.

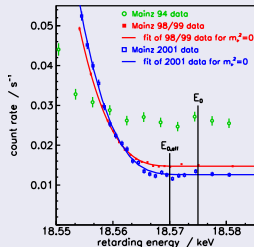
Mainz Experiment: solid  $^3\text{H}$  source (1997-2001)

$$m_\nu^2 = -0.6 \pm 2.2_{(\text{stat})} \pm 2.1_{(\text{sys})} \text{ eV}^2$$

$$\Downarrow$$

$$m_\nu < 2.3 \text{ eV (95\% C.L.) [8, 9]}$$

Results after all critical systematics measured  
(atomic physics, surface and solid state physics, inelastic scattering, self-charging, neighbour excitation)

Troitsk Experiment: gaseous  $^3\text{H}$  source (1997-2004)

$$m_\nu^2 = -0.67 \pm 1.89_{(\text{stat})} \pm 1.68_{(\text{sys})} \text{ eV}^2$$

$$\Downarrow$$

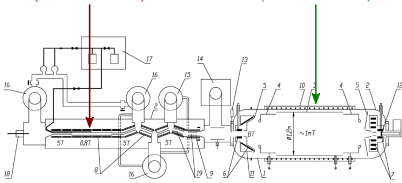
$$m_\nu < 2.05 \text{ eV (95\% C.L.) [7, 11]}$$

Most significant systematics:

- Stability of source conditions;
- Energy loss inside tritium source;
- Background due to non-optimal vacuum;

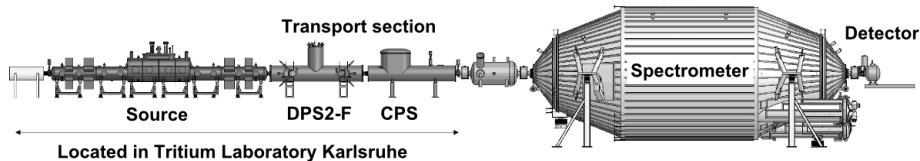
Windowless gaseous  $\text{T}_2$  source  
(similar to LANL)

MAC-E-Filter  
(similar to Mainz)



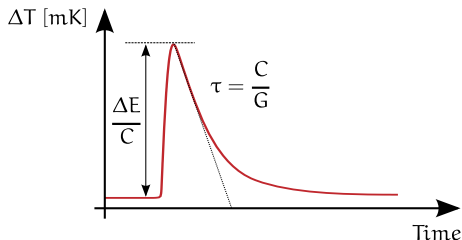
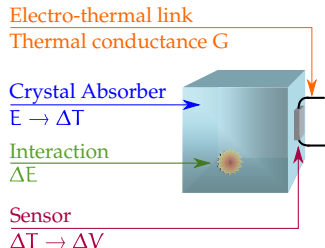


The KARlsruhe TRitium Neutrino Experiment (KATRIN)  
@ KIT (Karlsruhe Institute of Technology)



- Larger electrostatic spectrometer ever built (stainless steel vessel,  $\varnothing = 10$  m ,  $L = 22$  m);
- Intense Windowless Gaseous Tritium Source (WGTS):  $10^{11}$   $\beta$  decay electrons per second;
- Energy resolution:  $\Delta E = 0.93$  eV;
- High luminosity:  $L = 20$  cm<sup>2</sup> (Troitsk:  $L = 0.6$  cm<sup>2</sup>);
- Ultrahigh vacuum requirements:  $p < 10^{-11}$  mbar (to reduce the background).

Expected statistical sensitivity:  $m_\nu < 0.2$  eV @ 90% C.L. [12, 13]



- Complete energy thermalization: ionization, excitation  $\Rightarrow$  heat  $\Rightarrow$  calorimetry;
- $\Delta T = \frac{\Delta E}{C}$  where  $\Delta E$  is the released energy and  $C$  the total thermal capacity;
  - Absorber with very low thermal capacity:  $C \downarrow \Rightarrow \Delta T \uparrow$ ;
  - Debay law for superconductors below  $T_C$  and dielectric:  $C \propto \left(\frac{T}{\Theta_D}\right)^3$ ;
  - A very low temperature is needed:  $T \downarrow \Rightarrow C \downarrow \Rightarrow \Delta T \uparrow \Rightarrow (T = 10 \div 100 \text{ mK})$ ;
- Limit to energy resolution: statistical fluctuation of internal energy  $\Delta E_{\text{rms}} = \sqrt{k_B T^2 C}$ ;
- $\Delta T(t) = \frac{\Delta E}{C} e^{-t/\tau}$  with  $\tau = \frac{C}{G}$  and  $G$  thermal conductance.



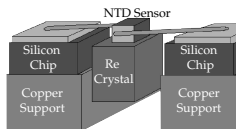
Isotope candidate:  $^{187}\text{Re} \beta \text{ decay} \Rightarrow ^{187}\text{Re} \rightarrow ^{187}\text{Os} + e^- + \bar{\nu}_e$

Rhenium is perfectly suited for fabricating thermal detectors.

- Dielectric or superconductor behaviour;
- Very low end point:  $Q = 2.47 \text{ keV}$ ;
- Half-life time:  $\tau_{1/2} = 43.2 \text{ Gy}$ ;
- High natural abundance: a.i. = 63%;
- Rate of 1 mg metallic Rhenium:  $\simeq 1.0 \text{ decay/s}$ .

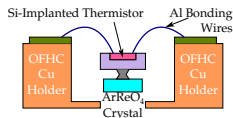
## Metallic Rhenium single crystals

- Absorber: Re superconductor with  $T_C = 1.6 \text{ K}$ ;
- Sensor: NTD thermistors;
- MANU experiment (Genova).



## Dielectric Rhenium compound ( $\text{AgReO}_4$ ) crystals

- Absorber:  $\text{AgReO}_4$  crystals (Silver perrhenate);
- Sensor: Silicon implanted thermistors;
- MIBETA experiment (Milano, Como, Trento).







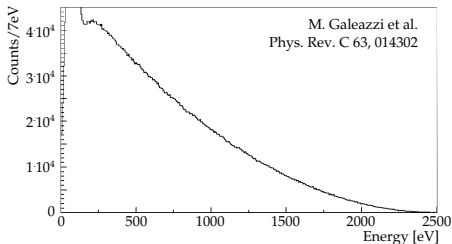
## MANU (1999)

- 1 crystal of metallic Re: 1.6 mg;
- $^{187}\text{Re}$  activity:  $\simeq 1.6$  Hz;
- Sensor: Ge NTD thermistor;
- Resolution:  $\Delta E = 96$  eV FWHM;
- Live-time: 0.5 years;
- $6.0 \cdot 10^6$   $^{187}\text{Re}$  decays above 420 eV.

$$m_{\nu}^2 = -462 \pm 579_{(\text{stat})} \pm 679_{(\text{sys})} \text{ eV}^2$$

 $\Downarrow$ 

$$m_{\nu} < 26 \text{ eV (95\% C.L.) [14]}$$



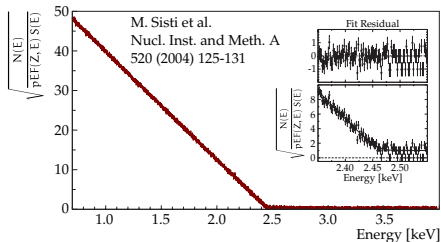
## MIBETA (2002-2003)

- 10  $\text{AgReO}_4$  crystals: 2.71 mg;
- $^{187}\text{Re}$  activity: 0.54 Hz/mg;
- Sensor: Si thermistor (ITC-irst now FBK);
- Resolution:  $\Delta E = 28.5$  eV FWHM;
- Live-time: 0.6 years;
- $6.2 \cdot 10^6$   $^{187}\text{Re}$  decays above 700 eV.

$$m_{\nu}^2 = -112 \pm 207_{(\text{stat})} \pm 90_{(\text{sys})} \text{ eV}^2$$

 $\Downarrow$ 

$$m_{\nu} < 15 \text{ eV (90\% C.L.) [15]}$$





## Exposure required for $m_\nu = 0.2$ eV sensitivity [16]

$A_\beta$ [Hz]	$\tau_{\text{rise}}$ [ $\mu\text{s}$ ]	$\Delta E$ [eV]	$N_{\text{ev}}$ [counts]	Exposure [det-year]
1	1	1	$0.2 \cdot 10^{14}$	$7.6 \cdot 10^5$
10	1	1	$0.7 \cdot 10^{14}$	$2.1 \cdot 10^5$
10	3	3	$1.3 \cdot 10^{14}$	$4.1 \cdot 10^5$
10	5	5	$1.9 \cdot 10^{14}$	$6.1 \cdot 10^5$
10	10	10	$3.3 \cdot 10^{14}$	$10.5 \cdot 10^5$

Example: red line in table (background  $b = 0$ )

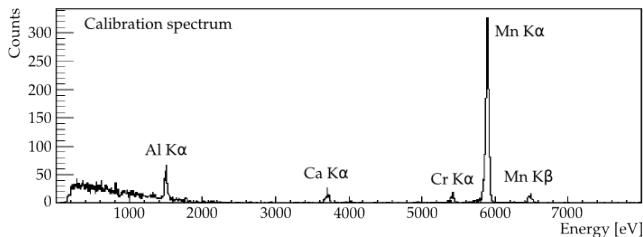
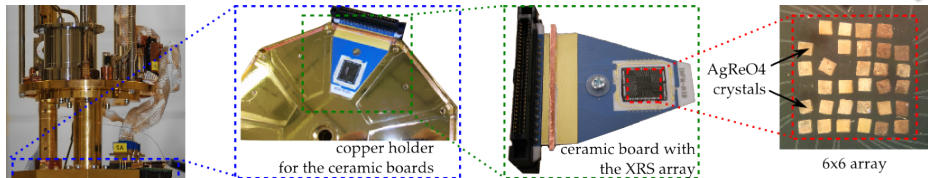
- 5000 pixels/array;
- 8 arrays;
- 10 years of live-time;
- 400 g  $^{\text{nat}}\text{Re}$ .

## Exposure required for $m_\nu = 0.1$ eV sensitivity [16]

$A_\beta$ [Hz]	$\tau_{\text{rise}}$ [ $\mu\text{s}$ ]	$\Delta E$ [eV]	$N_{\text{ev}}$ [counts]	Exposure [det-year]
1	0.1	0.1	$1.7 \cdot 10^{14}$	$5.4 \cdot 10^6$
10	0.1	0.1	$5.3 \cdot 10^{14}$	$1.7 \cdot 10^6$
10	1	1	$10.3 \cdot 10^{14}$	$3.3 \cdot 10^6$
10	3	3	$21.4 \cdot 10^{14}$	$6.8 \cdot 10^6$
10	5	5	$43.6 \cdot 10^{14}$	$13.9 \cdot 10^6$

Example: green line in table (background  $b = 0$ )

- 20000 pixels/array;
- 16 arrays;
- 10 years of live-time;
- 3.2 kg  $^{\text{nat}}\text{Re}$ .



- 31 AgReO<sub>4</sub> crystals glued on 1<sup>st</sup> array;
- Only 16 usable:  $\Delta E \simeq 47$  eV @ 2.6 keV,  $\tau_{\text{rise}} \simeq 1$  ms;
- **Not enough for improving previous  $m_{\nu}$  limits**  
 $\Rightarrow m_{\nu} \leq 10$  eV in 1 year of live time.



Status of Re detector development in about 20 years of test:

- To date no satisfactory results with Si- or Ge-thermistors but also with TES, MMCs;
- No clear understanding of Re absorber physics;
- Purity and superconductivity?
- Extra thermal capacity  $C$  due to nuclear quadrupole moment?
- low specific activity  $\Rightarrow$  need large mass to reach sub-eV sensitivity;
- systematics due to the Beta Environmental Fine Structure (BEFS);
- ... and due to the detector response function.

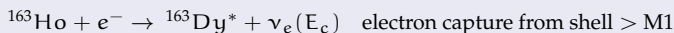
**AgReO<sub>4</sub> best detectors cannot provide the performances for sub-eV sensitivity**



with the current technologies the future of Re experiments is not very bright

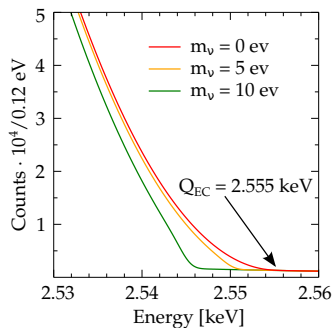
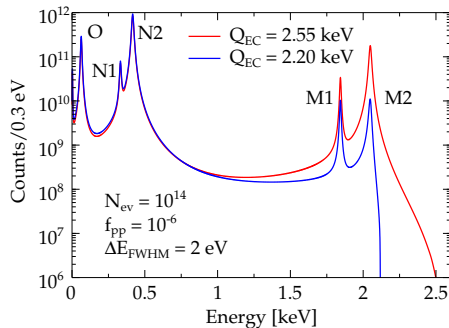


An interesting isotope suitable for the neutrino mass experiment could be the  $^{163}\text{Ho}$ .



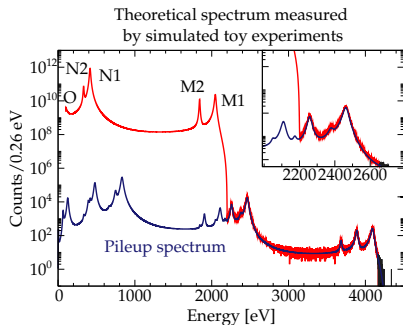
proposed by A. De Rujula e M. Lusignoli in 1982 [17, 18]

- Calorimetric measurement of Dy atomic de-excitations (mostly non-radiative):
  - ⇒ measurement of the entire energy released except the  $\nu$  energy;
- The rate at end-point may be as high as for  $^{187}\text{Re}$  but depends on  $Q_{\text{EC}}$ :
- $Q_{\text{EC}}$  and atomic de-excitation spectrum poorly known:
  - ⇒ Measured:  $Q_{\text{EC}} = (2.2 \div 2.8) \text{ keV}$ ;
  - ⇒ Recommended:  $Q_{\text{EC}} = 2.555 \text{ keV}$  [19, 20]);
- $\tau_{1/2} \simeq 4570 \text{ years} \Rightarrow$  high specific activity:
  - ⇒ Holmium detector not needed;
  - ⇒  $^{163}\text{Ho}$  can be implanted in any suitable microcalorimeter absorber;
- Complex pile-up spectrum;
- No high statistics and clean calorimetric measurement so far;



$$\frac{d\lambda_{EC}}{dE_c} = \frac{G_\beta^2}{4\pi^2} (Q_{EC} - E_c) \sqrt{(Q_{EC} - E_c)^2 - m_\nu^2} \times \sum_i n_i C_i \beta_i^2 B_i \frac{\Gamma_i}{2\pi} \frac{1}{(E_c - E_i)^2 + \Gamma_i^2/4}$$

- Continuum with marked peaks with Breit-Wigner shapes lines (width  $\Gamma_i$  of a few eV);
- Series of lines at the ionization energies  $E_i$  of the captured electrons;
- End-point shaped by  $\sqrt{(Q - E_e)^2 - m_\nu^2}$  (the same of the  $\beta$ -decay);
- Self calibrating spectrum;



$$S(E_c) = [N_{ev}(N_{EC}(E_c, m_\nu) + f_{pp} \times N_{EC}(E_c, 0) \otimes N_{EC}(E_c, 0)) + B(E_c)] \otimes R_{\Delta E}(E_c)$$

$N_{EC}(E_c, m_\nu)$  :  $^{163}\text{Ho}$  spectrum  
 $B(E)$  : background energy spectrum  
 $R_{\Delta E}(E_c)$  : detector energy response function

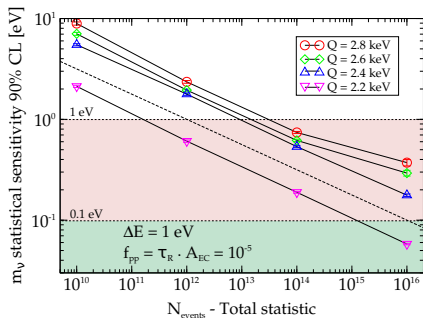
more details in A. Nucciotti, submitted to EPJC,  
arXiv:1405.5060 [21]

- Pulse pile-up occurs when multiple events arrive within the temporal resolving time of the detector;
- Unresolved pile-up produces a sort of background close to the end-point;
- The  $^{163}\text{Ho}$  pile-up events spectrum is quite complex and presents a number of peaks right at the end-point of the decay spectrum;
- To resolve pile-up:
  - Detector with fast signal rise-time  $\tau_{rise}$ ;
  - Pulse pile-up recovery algorithm



## Montecarlo Simulation

- $^{163}\text{Ho}$  production: neutron irradiation of Erbium (Er) enriched  $^{162}\text{Er}$ ;
- $^{163}\text{Ho}$  embedded in thermal detectors for low energy X-rays spectroscopy;
- Rate:  $2 \cdot 10^{11}$  nuclei of  $^{163}\text{Ho} \Rightarrow 1$  decay/s;



A. Nucciotti, submitted to EPJC, arXiv:1405.5060 [21]

## Requirements:

- High energy resolution ( $\simeq 1$  eV);
- Fast response detectors ( $\simeq 1$   $\mu\text{s}$ ) to avoid pile-up events;
- Multiplexable detectors array ( $\simeq 1000$ );



TESs, MMCs, MKIDs, ...



Exposure required for  $m_\nu = 0.2 \text{ eV}$  sensitivity [21, 22]

$A_\beta$ [Hz]	$\tau_{\text{rise}}$ [ $\mu\text{s}$ ]	$\Delta E$ [eV]	$N_{\text{ev}}$ [counts]	Exposure [det-year]
1	1	1	$2.8 \cdot 10^{13}$	$9.0 \cdot 10^5$
1	0.1	1	$1.3 \cdot 10^{13}$	$4.3 \cdot 10^5$
100	0.1	1	$4.6 \cdot 10^{13}$	$1.5 \cdot 10^4$
10	0.1	1	$2.8 \cdot 10^{13}$	$9.0 \cdot 10^4$
10	1	1	$4.6 \cdot 10^{13}$	$1.5 \cdot 10^5$

Example: green line in table (background  $b = 0$ )

- 5000 pixels/array;
- 3 arrays;
- 1 years of live-time;
- $2 \cdot 10^{17}$  nuclei of  $^{163}\text{Ho}$

Exposure required for  $m_\nu = 0.1 \text{ eV}$  sensitivity [21, 22]

$A_\beta$ [Hz]	$\tau_{\text{rise}}$ [ $\mu\text{s}$ ]	$\Delta E$ [eV]	$N_{\text{ev}}$ [counts]	Exposure [det-year]
1	0.1	0.3	$1.2 \cdot 10^{14}$	$3.9 \cdot 10^6$
100	0.1	0.3	$6.4 \cdot 10^{14}$	$2.0 \cdot 10^5$
100	0.1	1	$7.4 \cdot 10^{14}$	$2.4 \cdot 10^5$
10	0.1	1	$4.5 \cdot 10^{14}$	$1.5 \cdot 10^6$
10	1	1	$7.4 \cdot 10^{14}$	$2.4 \cdot 10^6$

Example: red line in table (background  $b = 0$ )

- 5000 pixels/array;
- 4 arrays;
- 10 years of live-time;
- $3 \cdot 10^{17}$  nuclei of  $^{163}\text{Ho}$

Exposure required for  $m_\nu = 0.2 \text{ eV}$  sensitivity [21, 22]

$A_\beta$ [Hz]	$\tau_{\text{rise}}$ [ $\mu\text{s}$ ]	$\Delta E$ [eV]	$N_{\text{ev}}$ [counts]	Exposure [det-year]
1	1	1	$0.2 \cdot 10^{14}$	$7.6 \cdot 10^5$
1	0.1	1	$1.6 \cdot 10^{15}$	$5.3 \cdot 10^7$
100	0.1	1	$9.8 \cdot 10^{15}$	$3.1 \cdot 10^6$
10	0.1	1	$3.8 \cdot 10^{15}$	$1.2 \cdot 10^7$
10	1	1	$9.8 \cdot 10^{15}$	$3.1 \cdot 10^7$

Example: green line in table (background  $b = 0$ )

- 60000 pixels/array;
- 5 arrays;
- 5 years of live-time;
- $4 \cdot 10^{18}$  nuclei of  $^{163}\text{Ho}$

Exposure required for  $m_\nu = 0.1 \text{ eV}$  sensitivity [21, 22]

$A_\beta$ [Hz]	$\tau_{\text{rise}}$ [ $\mu\text{s}$ ]	$\Delta E$ [eV]	$N_{\text{ev}}$ [counts]	Exposure [det-year]
1	0.1	0.3	$2.6 \cdot 10^{16}$	$8.2 \cdot 10^8$
100	0.1	0.3	$1.9 \cdot 10^{17}$	$5.9 \cdot 10^7$
100	0.1	1	$1.6 \cdot 10^{17}$	$5.0 \cdot 10^7$
10	0.1	1	$6.1 \cdot 10^{16}$	$1.9 \cdot 10^8$
10	1	1	$1.6 \cdot 10^{17}$	$5.0 \cdot 10^8$

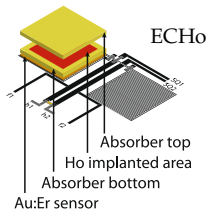
Example: red line in table (bkg=0)

- $10^6$  pixels/array;
- 6 arrays;
- 10 years of live-time;
- $8 \cdot 10^{19}$  nuclei of  $^{163}\text{Ho}$



## $^{163}\text{Ho}$ seems to be better than $^{187}\text{Re}$ :

- ☺ higher specific activity  $\Rightarrow$  Holmium detector not needed;
- ☺ self calibrating  $\Rightarrow$  better systematics control;
- ☹  $Q_{\text{EC}}$  and atomic de-excitation spectrum poorly known;
- ☹ complex pile-up spectrum;
- ☹ in case of higher  $Q \Rightarrow$  less sensitive;



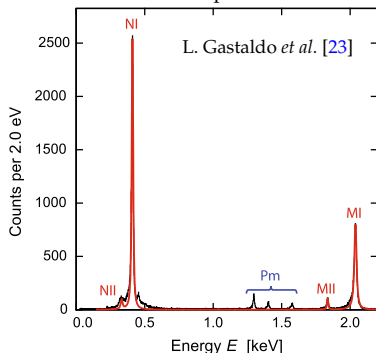
## (At least) two LTD projects with $^{163}\text{Ho}$ :

- ECHO, MMC detectors (Heidelberg)
- HOLMES, TES detectors (Milano, Genova, LNGS, NIST)
- Los Alamos Nat. Lab., Berkeley Univ., ...

## Common technical challenges:

- Clean  $^{163}\text{Ho}$  production;
- $^{163}\text{Ho}$  incorporation;
- Large channel number  $\Rightarrow$  high speed MUX;
- Data handling (processing, storage, ...)

Calorimetric spectrum of  $^{163}\text{Ho}$





## Goal

- Neutrino mass measurement:  
⇒  $m_\nu$  statistical sensitivity as low as 0.4 eV;
- Prove technique potential and its scalability (Megapixel experiment);
- assess EC Q-value;
- assess systematic errors;



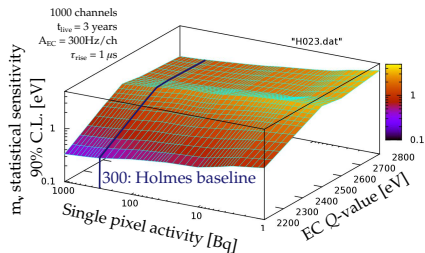
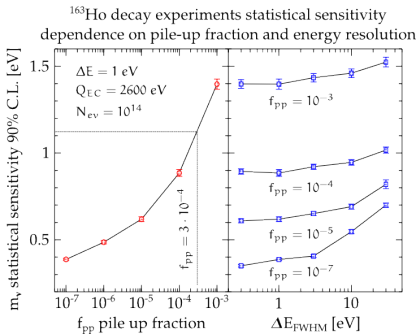
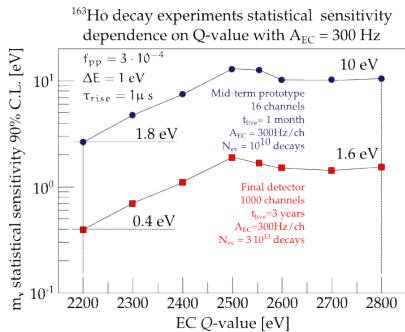
## Baseline

- Transition Edge Sensors (TES) with  $^{163}\text{Ho}$  implanted Bi:Au absorbers;
- $6.5 \cdot 10^{13}$  nuclei per detector ⇒ 300 dec/s;
- $\Delta E \simeq 1$  eV and  $\tau_{\text{rise}} \simeq 1$  s;
- 16 channel demonstrator/1000 channel final array;
- $3 \cdot 10^{13}$  events in 3 years;



Project Start: 1 Feb 2014

<http://artico.mib.infn.it/nucrimib/experiments/holmes>



- The experimental sensitivity is directly related to  $f_{pp} = \tau_{rise} \cdot A_{EC}$  (pile-up);
- The impact of the energy resolution is relatively smaller than that of pile-up;
- In presence of a high level of pile-up, the experiment is relatively less sensitive to the energy resolution;

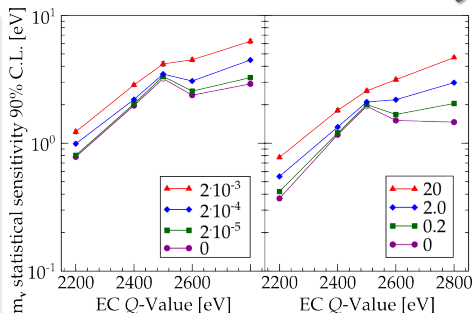


## Background sources:

- Environmental  $\gamma$  radiation:
  - Compton interactions;
  - Photoelectric interactions with photoelectron escape;
  - Fluorescent X-rays and X-ray escape lines;
- $\gamma$  and  $\beta$  from close surroundings;
- Cosmic rays at sea level (muons):
  - Au pixel:  $200 \times 200 \times 3 \mu\text{m}^3$   
 $\Rightarrow E \simeq 10 \text{ keV}, \text{rate} \simeq 1 \text{ d}^{-1}$ ;
  - Si chip:  $20 \times 20 \times 0.5 \text{ mm}^3$   
 $\Rightarrow E \simeq 300 \text{ keV}, \text{rate} \simeq 7000 \text{ d}^{-1}$ ;

## Experimental results:

- MIBETA:  $300 \times 300 \times 150 \mu\text{m}^3$  AgReO<sub>4</sub> crystals:  
 $\Rightarrow b(2.5\text{keV}) \simeq 1.5 \cdot 10^{-4} \text{ c/eV/d/det}$ ;
- TES @NIST (1600m):  $350 \times 350 \times 2.5 \mu\text{m}^3$  Bi absorbers:  
 $\Rightarrow b < 1 \text{ c/eV/d/det}$  (preliminary);



A constant background  $b$  is negligible if it is much smaller than the pile-up spectrum

$$b \ll \frac{A_{EC} \cdot f_{pp}}{2Q_{EC}}$$

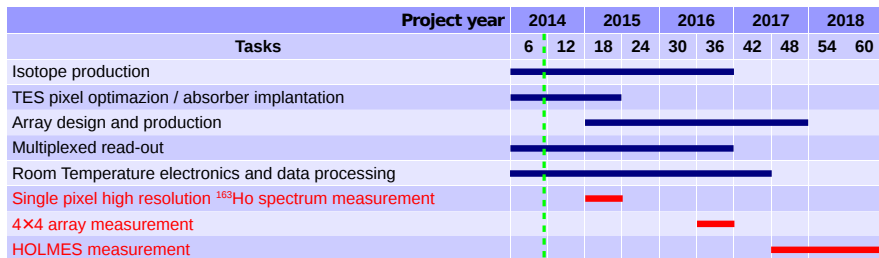
For large activities  $A_{EC}$ , and correspondingly large pile-up rate, the statistical sensitivity should be relatively insensitive to cosmic rays and to environmental radioactivity.



- $^{163}\text{Ho}$  isotope production;
- $^{163}\text{Ho}$  isotope embedding in detector;
- Single TES optimization and testing;
- TES array design, engineering and testing;
- SQUID read-out and multiplexing optimization and testing (rf-SQUID);
- Real time and offline signal processing and analysis (trigger, OF filter, pile-up rejection);
- Cryogenic set-up (new LHe-free cryostat, pulse-tube assisted);

Development in two steps:

- First demonstrator prototype: 16 pixel prototype;
- Final detector array: 1000 pixel;





## Neutron reactor activation:

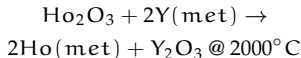
Enriched  $^{162}\text{Er}$  targets for indirect production of  $^{163}\text{Ho}$



- Requires  $^{162}\text{Er}$  enrichment (nat i.a.=0.139%) and oxide chemical form ( $\text{Er}_2\text{O}_3$ );
- $3 \cdot 10^{12}$   $^{163}\text{Ho}$  nuclei/mg( $^{162}\text{Er}$ )/h for a thermal flux of  $10^{13}$  n/cm<sup>2</sup>/s;
- Not all cross sections are known: the process will be studied;
- Unavoidable  $^{166\text{m}}\text{Ho}$ :  $^{165}\text{Ho}(n, \gamma)^{166\text{m}}\text{Ho}$  ( $\beta$ ,  $t_{1/2} = 1200$  y) from Ho contaminations or  $^{164}\text{Er}(n, \gamma)$ ;
- Unavoidable  $^{164}\text{Ho}$ : fast neutron activation  $^{163}\text{Ho}(n, \gamma)^{164}\text{Ho}$

<b>Tm 163</b> 1.81 h $\epsilon$ $\beta^+$ $\gamma$ 104; 69; 241; 1434; 1397	<b>Tm 164</b> 6.1 m 2.8 m $\epsilon$ $\beta^+$ 2.9 $\gamma$ 206; 1158; 267; 807	<b>Tm 165</b> 30.06 h $\epsilon$ $\beta^+$ $\gamma$ 243; 47; 297; 807	<b>Tm 166</b> 7.70 h $\epsilon$ $\beta^+$ 1.9 $\gamma$ 779; 2052; 184; 1274...	<b>Tm 167</b> 9.25 d $\epsilon$ $\beta^+$ 532...	<b>Tm 168</b> 93.1 d $\epsilon$ $\beta^+$ $\gamma$ 198; 816; 447
<b>Er 162</b> 0.139 $\alpha$ 19 $\sigma_{\text{th}, \alpha} < 0.011$	<b>Er 163</b> 75 m $\beta^+$ $\gamma$ (1114...)	<b>Er 164</b> 1.601 $\alpha$ 13 $\sigma_{\text{th}, \alpha} < 0.0012$	<b>Er 165</b> 10.3 h $\epsilon$ $\beta^+$ $\gamma$ no $\gamma$	<b>Er 166</b> 33.503 $\alpha$ 5 + 14 $\sigma_{\text{th}, \alpha} < 7\text{E-5}$	<b>Er 167</b> 2.3 s 22.889 $\beta^-$ 200 $\sigma_{\text{th}, \beta^-} < 3\text{E-6}$
<b>Ho 161</b> 5.7 a $\alpha$ 28; 76; h 211	<b>Ho 162</b> 68 m 15 m h 56; 36 $\beta^+$ 1.1 $\gamma$ 185; 1620; 283; 1319	<b>Ho 163</b> 1.1 a 4570 a h 37; 31; 67; 73	<b>Ho 164</b> 37 m 29 m $\beta^-$ 3.1 + 58 $\sigma_{\text{th}, \beta^-} < 2\text{E-5}$	<b>Ho 165</b> 100 $\beta^-$ 107 1200 a 23.80 h $\gamma$ 184; 810; 719 $\gamma$ 81; $\epsilon$ 3150	<b>Ho 166</b> 1.3 m 2.35 h $\beta^-$ 1.3 1.3; $\gamma$ 26; 1.915; 1762; J $\epsilon$ 3305
<b>Dy 160</b> 2.329 $\alpha$ 60 $\sigma_{\text{th}, \alpha} < 0.0003$	<b>Dy 161</b> 18.889 $\alpha$ 600 $\sigma_{\text{th}, \alpha} < 1\text{E-6}$	<b>Dy 162</b> 25.475 $\alpha$ 170	<b>Dy 163</b> 24.896 $\alpha$ 120 $\sigma_{\text{th}, \alpha} < 2\text{E-5}$	<b>Dy 164</b> 28.260 $\alpha$ 1610 + 1040	<b>Dy 165</b> 1.3 m 2.35 h $\beta^-$ 1.3 1.3; $\gamma$ 26; 1.915; 1762; J $\epsilon$ 3305
<b>Tb 159</b> 100	<b>Tb 160</b> 72 d 2.3 d	<b>Tb 161</b> 6.90 d	<b>Tb 162</b> 7.78 m	<b>Tb 163</b> 10.5 m	<b>Tb 164</b> 9.0 m

Thermoreduction to obtain the metallic Ho target for implantation:





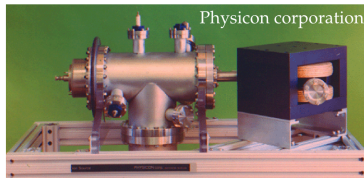
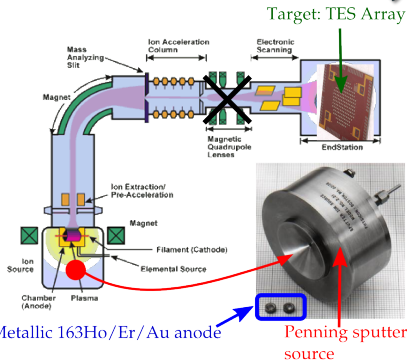


## Implant procedure:

- magnetic mass separation to separate  $^{163}\text{Ho}$  from Dy, Er and more;
- $^{163}\text{Ho}$  embedding in the detector absorber;

## Ion implanter:

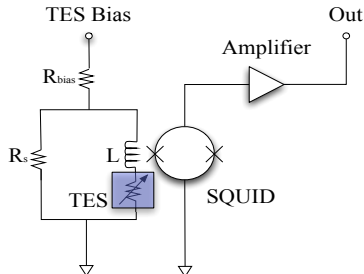
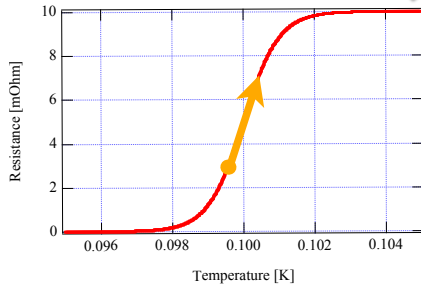
- Ionic source: Penning sputter source with metallic  $^{163}\text{Ho}/\text{Er}/\text{Au}$  anode;
- Mass-analysis magnet for ion beam extracted from the ion source;
- Acceleration mechanics: ions electrostatically accelerated to a high energy;
- Target chamber: ions ( $^{163}\text{Ho}$ ) impinge on a target (TES absorber, Au);
- $20 \div 30 \text{ KeV}$  for  $50 \div 100 \text{ nm}$  penetration in Au;





**Transition Edge Sensor (TES):** cryogenic particle detector that exploits the strongly temperature-dependent resistance of the superconducting phase transition.

- Superconductor biased in its transition;
- "Self-biased region"  $\Rightarrow$  the power dissipated in the device is constant with the applied bias;
- Electrothermal feedback: if  $R_{TES} \uparrow \Rightarrow I_{TES} \downarrow \Rightarrow P_J \downarrow \Rightarrow$  cooling the device back to its equilibrium state in the self-biased region;
- Low resistance: read out with SQUIDs (Superconducting Quantum Interference Devices);
- TES operates in series with the input coil  $L$  which is inductively coupled to a SQUID series-array;
- Change in TES current  $\Rightarrow$  change in the input flux to the SQUID;
- The SQUID output is further amplified and read by room-temperature electronics;

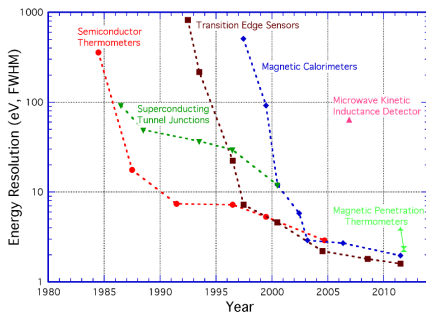




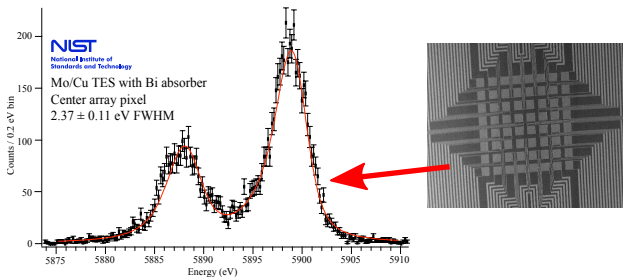
- Strongly supported by the X-ray astrophysics community for the past couple of decades (but also Dark Matter and rare events research);
- Small size  $\Rightarrow$  low thermal capacity  $C \Rightarrow$  excellent energy resolution:

$$\Delta E_{FWHM} = \begin{cases} 1.26 \text{ eV @ } 1.5 \text{ keV} \\ 1.58 \text{ eV @ } 6 \text{ keV} \\ 1.94 \text{ eV @ } 8 \text{ keV} \end{cases}$$

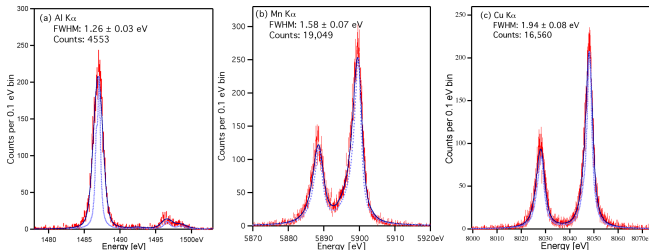
- The negative electro-thermal feedback provides a fast time response;
- Large Array and multiplexing (TDM, CDM and FDM);
- Cross-talk between pixels less than 0.01%;
- Tunable critical temperature  $T_C$  exploiting the proximity effect [24]  $\Rightarrow$  Mo:Cu or Mo:Au proximity TES ( $T_C \simeq 100 \text{ mK}$ );

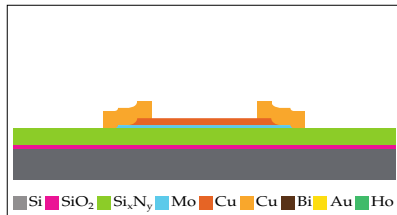


TESs are natural candidates to reach an energy resolution of 1 eV and a time resolution of 1  $\mu$ s



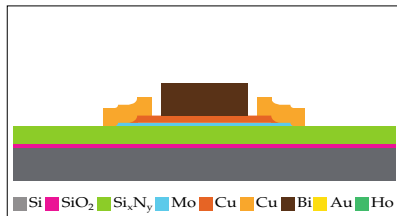
## NASA/Goddard Space Flight Center





### Phase 1 @NIST

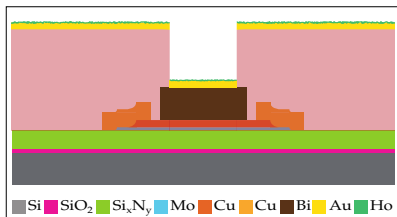
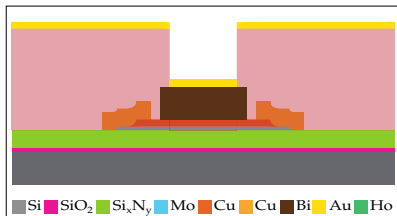
- Mo:Cu proximity TES ( $T_C \simeq 100$  mK) [24];
- SiO<sub>2</sub> stopper layer;
- Si<sub>x</sub>N<sub>y</sub> membrane for thermal insulation;
- deposited on a Si substrate.



### Phase 2 @NIST

Bismuth deposition for the first absorber layer ( $2 \div 4 \mu\text{m}$ ) by lift-off process:

- Photoresist deposition (sacrificial layer);
- Target material (Bi) deposition;
- Wash out of the sacrificial layer;



### Phase 3 @NIST

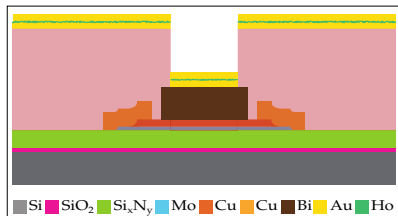
Gold deposition for the second absorber layer  
(0.1 ÷ 0.2 μm):

- Lift-off not finished (no photoresist wash out);
- Ship to Genova (for the  $^{163}\text{Ho}$  implant);

### Phase 4 @Genova

$^{163}\text{Ho}$  implanting:

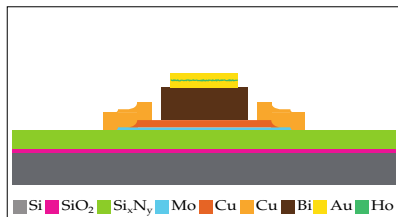
- Metallic  $^{163}\text{Ho}/\text{Er}/\text{Au}$  anode (source);
- Magnetic mass separation;
- Implantation and magnetic separation;



### Phase 5 @Genova

Gold film deposition for full containment:

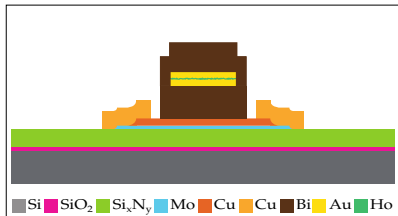
- <sup>163</sup>Ho coating with thin Au (0.1 ÷ 0.2 m) layer;



### Phase 6 @Genova

Lift-off of the Au:Ho:Cu layer:

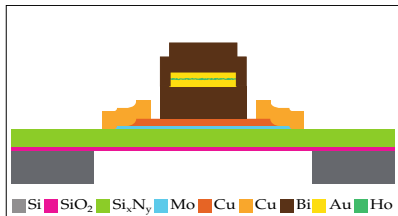
- <sup>163</sup>Ho-implanted Au-absorber.



### Phase 7 @Genova

Second Bi absorber layer (2 ÷ 4 m):

- Bi fully encapsulates Au:Ho layer;

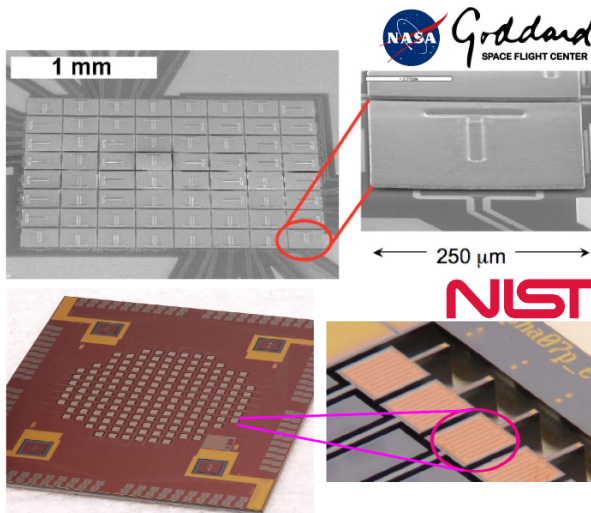


### Phase 8 @Genova (final fabrication phase)

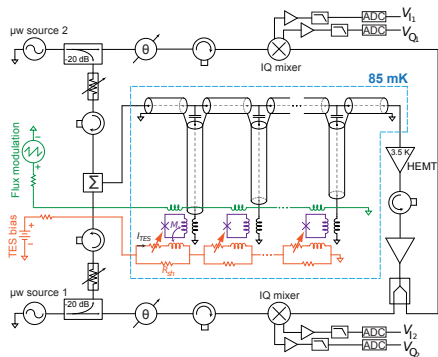
Deep reactive ion etching (DRIE) to remove Si substrate (and to achieve necessary thermal isolation):

- Suspended TES with Bi:Cu absorber <sup>163</sup>Ho-implanted (T-shaped);
- Ship to Milano;
- Installation in the Cryogenics facility;

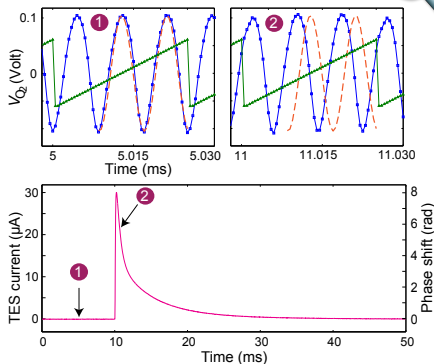




NIST design is the starting point for the HOLMES array detector:  $4 \times 256$  pixel



- DC biased TES (1 bias for all TESs);
- SQUID coupled with TES and a resonator circuit;
- Microwave rf-SQUID read out with flux ramp modulation (common flux line is inductively coupled to all the SQUIDs);
- Signal reconstructed by homodyne detection (IQ signal de-multiplexing) and demodulation;



- 2 Channels demonstrator @NIST [25];
- Bandwidth/pixel 10MHz  $\Rightarrow$  50 resonances between 0 and 500MHz (typical commercial ADC range);



- Reconfigurable Open Architecture Computing Hardware (ROACH) designed by the Collaboration For Astronomy Signal Processing and Electronics Research (CASPER);
- Xilinx Virtex FPGA based digital data processing;
- Frequency comb generation ( $\simeq 60$  tones in the  $0 \div 550$  MHz range);
- Quadrature frequency upmixing (500 MHz  $\rightarrow$  5 GHz) and down-mixing (5 GHz  $\rightarrow$  500 MHz);
- Signal channelizing and rf-SQUID signal de-modulation
- Real time signal processing;
- Strongly tested for MKIDs read-out (ARCONS, 2048 pixels);

IF Board                      ADC/DAC Board                      ROACH2

## Design for HOLMES:

- $4 \times 256 = 1024$  pixels;
- Target: 64 resonance per ROACH-module;
- Complete system composed by 16 module.



- The measurement of the end point of nuclear beta or electron capture (EC) decays spectra is the only model-independent;
- The goal of the next generation experiments is the sub-eV neutrino mass sensitivity;
- The HOLMES experiment will perform a direct measurement of the neutrino mass by using microcalorimeter with absorber  $^{163}\text{Ho}$ -implanted;
- The Goals of the HOLMES experiment are:
  - assess EC Q-value of the  $^{163}\text{Ho}$ ;
  - assess systematic errors;
  - reach a statistical sensitivity as low as 0.4 eV;
  - prove technique potential and its scalability (Megapixel experiment);



- [1] F. Capozzi, G.L. Fogli, E. Lisi, A. Marrone, D. Montanino et al., “**Status of three-neutrino oscillation parameters, circa 2013**”, 2013, e-print: [arXiv:1312.2878](#) [hep-ph].
- [2] Stefano Dell’Oro, Simone Marcocci and Francesco Vissani, “**New expectations and uncertainties on Neutrinoless Double Beta Decay**”, 2014, e-print: [arXiv:1404.2616](#) [hep-ph].
- [3] Srubabati Goswami, Abhijit Bandyopadhyay and Sandhya Choubey, “**Global analysis of neutrino oscillation**”, *Nuclear Physics B - Proceedings Supplements*, vol. 143, no. 0, no. 0, pp. 121 – 128, 2005, doi:10.1016/j.nuclphysbps.2005.01.096.
- [4] Mark Wyman, Douglas H. Rudd, R. Ali Vanderveld and Wayne Hu, “ **$\nu \Lambda$ CDM: Neutrinos help reconcile Planck with the Local Universe**”, *Phys.Rev.Lett.*, vol. 112, p. 051302, 2014, doi:10.1103/PhysRevLett.112.051302, e-print: [arXiv:1307.7715](#) [astro-ph.CO].
- [5] M. Agostini et al. (GERDA Collaboration), “**Results on Neutrinoless Double- $\beta$  Decay of  $^{76}\text{Ge}$  from Phase I of the GERDA Experiment**”, *Phys. Rev. Lett.*, vol. 111, no. 12, no. 12, p. 122503, 2013, doi:10.1103/PhysRevLett.111.122503, e-print: [arXiv:1307.4720](#) [nucl-ex].
- [6] J.B. Albert et al. (EXO-200 Collaboration Collaboration), “**Search for Majorana neutrinos with the first two years of EXO-200 data**”, 2014, e-print: [arXiv:1402.6956](#) [nucl-ex].



- [7] V.M Lobashev et al., “**Direct search for neutrino mass and anomaly in the tritium beta-spectrum: Status of troitsk neutrino mass experiment**”, *Nucl. Phys. B. (Proc. Suppl.)*, vol. 91, no. 13, no. 13, pp. 280–286, 2001, doi:10.1016/S0920-5632(00)00952-X.
- [8] Ch. Kraus et al., “**Final results from phase II of the Mainz neutrino mass search in tritium  $\beta$  decay**”, *Eur. Phys. J. C*, vol. 40, no. 4, no. 4, pp. 447–468, 2005, doi:10.1140/epjc/s2005-02139-7.
- [9] Christine Kraus, Andrej Singer, Kathrin Valerius and Christian Weinheimer, “**Limit on sterile neutrino contribution from the Mainz Neutrino Mass Experiment**”, *Eur. Phys. J. C*, vol. 73, p. 2323, 2013, doi:10.1140/epjc/s10052-013-2323-z, e-print: [arXiv:1210.4194](https://arxiv.org/abs/1210.4194) [hep-ex].
- [10] A. Picard et al., “**A solenoid retarding spectrometer with high resolution and transmission for keV electrons**”, *Nuclear Instruments and Methods in Physics Research Section B: Beam Interactions with Materials and Atoms*, vol. 63, no. 3, no. 3, pp. 345 – 358, 1992, doi:10.1016/0168-583X(92)95119-C.
- [11] V.N. Aseev et al. (Troitsk Collaboration Collaboration), “**An upper limit on electron antineutrino mass from Troitsk experiment**”, *Phys.Rev. D*, vol. 84, p. 112003, 2011, doi:10.1103/PhysRevD.84.112003, e-print: [arXiv:1108.5034](https://arxiv.org/abs/1108.5034) [hep-ex].
- [12] J. Angrik et al., “**KATRIN design report 2004**”, *Tech. Rep., Forschungszentrum, Karlsruhe, Germany*, pp. 447–468, 2004.  
NPI ASCR Řež, EXP-01/2005, FZKA Scientific Report 7090, MS-KP-0501.



- [13] Michael Sturm, “**Status of the KATRIN experiment with special emphasis on source-related issues**”, 2011, e-print: [arXiv:1111.4773 \[hep-ex\]](#).
- [14] M. Galeazzi, F. Fontanelli, F. Gatti and S. Vitale, “**End-point energy and half-life of the  $187\text{re}$   $\beta$  decay**”, *Phys. Rev. C*, vol. 63, p. 014302, 2000, doi:10.1103/PhysRevC.63.014302.
- [15] M. Sisti, et al., “**New limits from the milano neutrino mass experiment with thermal microcalorimeters**”, *Nuclear Instruments and Methods in Physics Research Section A: Accelerators, Spectrometers, Detectors and Associated Equipment*, vol. 520, no. 13, no. 13, pp. 125–131, 2004, doi:10.1016/j.nima.2003.11.273.
- [16] A. Nucciotti, E. Ferri and O. Cremonesi, “**Expectations for a new calorimetric neutrino mass experiment**”, *Astropart.Phys.*, vol. 34, pp. 80–89, 2010, doi:10.1016/j.astropartphys.2010.05.004, e-print: [arXiv:0912.4638 \[hep-ph\]](#).
- [17] A. De Rujula and M. Lusignoli, “**Calorimetric measurements of  $163\text{holmium}$  decay as tools to determine the electron neutrino mass**”, *Physics Letters B*, vol. 118, no. 46, no. 46, pp. 429–434, 1982, doi:10.1016/0370-2693(82)90218-0.
- [18] A. de Rujula and M. Lusignoli, “**Single electron ejection in electron capture as a tool to measure the electron neutrino mass**”, *Nuclear Physics B*, vol. 219, no. 2, no. 2, pp. 277 – 301, 1983, doi:10.1016/0550-3213(83)90642-9.



- [19] C.W. Reich and Balraj Singh, “**Nuclear data sheets for  $a = 163$** ”, *Nuclear Data Sheets*, vol. 111, no. 5, no. 5, pp. 1211 – 1469, 2010, doi:10.1016/j.nds.2010.04.001.
- [20] G. Audi, A.H. Wapstra and C. Thibault, “**The ame2003 atomic mass evaluation: (ii). tables, graphs and references**”, *Nuclear Physics A*, vol. 729, no. 1, no. 1, pp. 337 – 676, 2003, doi:j.nuclphysa.2003.11.003.  
The 2003 NUBASE and Atomic Mass Evaluations.
- [21] A. Nucciotti, “**Statistical sensitivity of 163-Ho electron capture neutrino mass experiments**”, 2014, e-print: [arXiv:1405.5060](https://arxiv.org/abs/1405.5060) [physics.ins-det].
- [22] Massimiliano Galeazzi, Flavio Gatti, Maurizio Lusignoli, Angelo Nucciotti and Stefano Ragazzi, “**The Electron Capture Decay of 163-Ho to Measure the Electron Neutrino Mass with sub-eV Accuracy and Beyond**”, *submitted to Physical Review D*, 2012, e-print: [arXiv:1202.4763](https://arxiv.org/abs/1202.4763) [physics.ins-det].
- [23] L. Gastaldo et al., “**The Electron Capture 163Ho Experiment ECHO**”, *Journal of Low Temperature Physics*, 2014, doi:10.1007/s10909-014-1187-4.
- [24] Hans Meissner, “**Superconductivity of contacts with interposed barriers**”, *Physical Review*, vol. 117, pp. 672–680, February 1960, doi:10.1103/PhysRev.117.672.





- [25] Omid Noroozian et al., “**High-resolution gamma-ray spectroscopy with a microwave-multiplexed transition-edge sensor array**”, *Applied Physics Letters*, vol. 103, no. 20, no. 20, 2013, doi:<http://dx.doi.org/10.1063/1.4829156>.